Blockade of AT1 Receptor Reduces Apoptosis, Inflammation, and Oxidative Stress in Normotensive Rats with Intracerebral Hemorrhage[S]

Keun-Hwa Jung, Kon Chu, Soon-Tae Lee, Se-Jeong Kim, Eun-Cheol Song, Eun-Hee Kim, Dong-Kyu Park, Dong-In Sinn, Jeong-Min Kim, Manho Kim, and Jae-Kyu Roh

Stroke and Neural Stem Cell Laboratory, Department of Neurology, Clinical Research Institute, Seoul National University Hospital, Seoul, Republic of Korea (K.-H.J., K.C., S.-T.L., S.-J.K., E.-C.S., E.-H.K., D.-K.P., D.-I.S., J.-M.K., M.K., J.-K.R.); Program in Neuroscience, Neuroscience Research Institute of Seoul National University Medical Research Center, Seoul National University, Seoul, Republic of Korea (K.-H.J., K.C., S.-T.L., D.-I.S., M.K., J.-K.R.); and Division of Epidemic Intelligence Service, Korea Center for Disease Control and Prevention, Seoul, Republic of Korea (K.-H.J.)

ABSTRACT

Angiotensin II exerts its central nervous system effects primarily via its receptors AT1 and AT2, and it participates in the pathogenesis of ischemia via AT1. The selective AT1 receptor blocker (ARB) is used in the hypertension treatment, and it exerts a variety of pleiotropic effects, including antioxidative, antiapoptotic, and anti-inflammatory effects. In this study, we investigated the therapeutic effect of the ARB telmisartan in experimental intracerebral hemorrhage (ICH) in normotensive rats. ICH was induced via the collagenase infusion or autologous blood injection. Either telmisartan at 30 mg/kg/dose or phosphate-buffered saline was orally administered 2 h after ICH induction. We evaluated hemorrhage volume, brain water content, and functional recovery, and we performed the histological analysis for terminal deoxynucleotidyl transferase dUTP nick-end labeling, leukocyte infiltration, and microglia activation. A variety of intracellular signals, in terms of oxidative stress, apoptotic molecules, and inflammatory mediators, were also measured. Telmisartan reduced hemorrhage volume, brain edema, and inflammatory or apoptotic cells in the perihematomal area. Telmisartan was noted to induce the expression of endothelial nitric-oxide synthase and peroxisome proliferator-activated receptor γ and decrease oxidative stress, apoptotic signal, tumor necrosis factor-α, and cyclooxygenase-2 expression. The telmisartan-treated rats exhibited less pronounced neurological deficits and recovered better. Thus, telmisartan seems to offer neural protection, including antiapoptosis, anti-inflammatory, and antioxidant benefits in the intracerebral hemorrhage rat model.

Angiotensin II is a potent vasoconstrictor hormone that is cleaved from angiotensinogen by renin and angiotensin-converting enzyme. In addition to its known vital role in both cardiovascular and fluid homeostasis, several lines of evidence implicate angiotensin II in the ischemic neuronal injury via the angiotensin II receptor subtype AT1 (AT1R) (Walther et al., 2002). Emerging evidence suggest that pe-

ripherally administered AT1R blockers (ARBs) can interact with AT1R in the brain across the blood-brain barrier (BBB) and reduce the infarct volumes in the experimental cerebral ischemia model (Dai et al., 1999; Nishimura et al., 2000; Yamakawa et al., 2003). Recently, ARBs were also proven to attenuate inflammatory and oxidative stress (Ando et al., 2004; Zhou et al., 2005) and to regulate the nitric-oxide synthase isoenzymes in the brain (Ito et al., 2002). As a potent and highly selective AT1 receptor antagonist, telmisartan (TMS) is described chemically as 4[(1,4-dimethyl-2-propyl[2,6-bi-1*H*-benzimidazol]-1-yl)methyl] [1,1-biphenyl]-2-carboxylic acid. This unique feature of telmisartan accounts for both its high receptor affinity and its excellent pharmacokinetic properties. Furthermore, telmisartan could

ABBREVIATIONS: AT1R, angiotensin II receptor subtype AT1; ARB, angiotensin II receptor blocker; BBB, blood brain barrier; TMS, telmisartan; PPAR, peroxisome proliferator-activated receptor; ICH, intracerebral hemorrhage; MLPT, modified limb placing test; MPO, myeloperoxidase; TUNEL, terminal deoxynucleotidyl transferase dUTP nick-end labeling; eNOS, endothelial nitric-oxide synthase; COX, cyclooxygenase; RT-PCR, reverse transcription-polymerase chain reaction; FasL, Fas ligand; TNF, tumor necrosis factor; DHE, dihydroethidium; MDA, malondialdehyde; ANOVA, analysis of variance; NF-κB, nuclear factor-κB.

confer effects other than the blockage of the AT1R, such as peroxisome proliferator-activated receptor (PPAR) γ activation (Benson et al., 2004).

The neurotoxicity associated with intracerebral hemorrhage (ICH) includes inflammation, oxidative stress, and excitotoxicity, as well as toxic effects of blood degradation products (Wang et al., 2002; Chu et al., 2004; Jung et al., 2004; Lee et al., 2006). Recent work has indicated that the suppression of these responses can reduce brain edema and improve functional outcomes in experimental ICH (Mayne et al., 2001; Peeling et al., 2001; Chu et al., 2004; Jung et al., 2004; Lee et al., 2006). Given that angiotensin II is the principal inducer of oxidative stress and inflammation (Rajagopalan et al., 1996; Iadecola and Gorelick, 2004; Chalupsky and Cai, 2005), the acute blockade of AT1R might exert beneficial effects in the hemorrhagic brain. However, to date, there was no study validating the effects of ARB as a potential therapeutic agent against ICH.

Peripherally administered telmisartan penetrates the BBB to inhibit the central effects of angiotensin II via selective blockage of AT1R, but not AT2R (Gohlke et al., 2001). Since high doses of the antagonist, i.e., 10 mg/kg i.v. and 30 mg/kg p.o., could result in the nearly complete and sustained blockade of AT1R within the brain (Gohlke et al., 2001), we attempted to study the therapeutic effects of a high dose of telmisartan in normotensive rats in which ICH had been induced.

Materials and Methods

Induction of Intracerebral Hemorrhage and Telmisartan Treatment. All the procedures were performed following institutional approval in accordance with National Institutes of Health *Guide for the Care and Use of Laboratory Animals* (Institute of Laboratory Animal Resources, 1996). Male Sprague-Dawley rats (12 weeks old; Orient, Seoul, Republic of Korea), weighing 200 to 220 g, were randomly assigned to two experimental groups: ICH-vehicle group (ICH-only) and telmisartan-treated ICH group (ICH-TMS). Experimental ICH was induced via stereotaxic intrastriatal administration of bacterial collagenase type VII (Sigma-Aldrich, St. Louis, MO), as has been described in other reports (Chu et al., 2004; Jung et al., 2004; Lee et al., 2006). Two hours after ICH induction, a single oral dose of telmisartan (30 mg/kg/dose p.o., dissolved in 1 ml of PBS; GlaxoSmithKline, Seoul, Korea) was administered to the rats by feeding tubes. An equal amount of PBS was administered to the ICH-only group. We measured mean arterial blood pressure and arterial blood gases via a right femoral artery line (polyethylene 50 tubing). A small amount of heparinized saline was used to prevent clotting in the femoral artery and catheter. Physiological parameters were assessed 30 min before and after ICH induction and 6 and 24 h after telmisartan (or PBS) administration.

Autologous Blood-Injected ICH Model. Additional experiments were also performed using a direct infusion of autologous blood into the rat striatum as an alternative model (Chu et al., 2004; Lee et al., 2006). A small craniotomy was performed using the same stereotactic coordinates, and 300 μl of autologous unheparinized blood (from the femoral artery) was infused into the left striatum. In this model, we analyzed the brain water content in the ICH-only group and ICH-TMS group (30 mg/kg) that were initially treated 2 h after ICH induction, and we verified whether the effects of telmisartan would be comparable with those in the collagenase-induced ICH models.

Behavioral Testing. To examine the effects of the telmisartan on the neurological deficits of rats after ICH, behavioral tests were performed by two investigators blinded to the treatment status of the

rats, with the modified limb placing test (MLPT) (Chu et al., 2004; Jung et al., 2004; Lee et al., 2006). The test consists of two limb-placing tasks that assess the sensorimotor integration of the forelimb and the hind limb by checking responses to tactile and proprioceptive stimulation. First, the rat is suspended 10 cm over a table, and the stretch of the forelimbs toward the table is observed and evaluated: normal stretch, 0 points; and abnormal flexion, 1 point. Next, the rat is positioned along the edge of the table, with its forelimbs suspended over the edge, and it is allowed to move freely. Each forelimb (forelimb, second task; and hind limb, third task) is gently pulled down, and retrieval and placement are checked. Finally, the rat is placed toward the table edge to check for lateral placement of the forelimb. The three tasks are scored in the following manner: normal performance, 0 points; performance with a delay (2 s) and/or incomplete, 1 point; and no performance, 2 points. In total, 7 points means maximal neurological deficit, and 0 points means normal performance. The animals were monitored during the period of postoperative recovery starting at 2 h and 1, 7, 14, 21, and 28 days after ICH ($n = 6$/group).

Hemorrhage Volume and Water Content. Hemorrhage volume was quantified at 24 or 72 h via a spectrophotometric assay conducted as described previously (Lee et al., 2006). Measurements from perfused brains subjected to ICH were compared with the standard curve to obtain data in terms of hemorrhage volume (microliters; $n = 6$/group). Seventy-two hours after the induction of ICH, the rats were anesthetized, sacrificed via decapitation, and processed for measuring water content ($n = 6$/group) (Chu et al., 2004; Jung et al., 2004; Lee et al., 2006). Water content was expressed as a percentage of wet weight.

Tissue Preparation and Immunohistochemistry. On day 3, the rats ($n = 6$/group) were reanesthetized and perfused through the heart with 50 ml of ice-cold saline and 50 ml of 4% paraformaldehyde, in 0.1 M PBS. We conducted immunostaining with antibodies against myeloperoxidase (MPO; 1:200; Dako, Carpinteria, CA), and OX42 (1:500; Chemicon International, Temecula, CA), as described previously (Chu et al., 2004; Jung et al., 2004; Lee et al., 2006). We also conducted a TUNEL procedure for the in situ detection of DNA fragmentation, as was described previously (Chu et al., 2004; Jung et al., 2004; Lee et al., 2006). Coronal sections taken through the center of the needle insertion were analyzed via the counting of marker-specific cells throughout the entire section (three sections per each antibody staining; 1 mm in width). The total counts in these sections were converted to cell densities to facilitate quantitation and comparison between the groups.

Western Blotting. Twenty-four hours after the induction of ICH, the rats were sacrificed via decapitation, and the brains were immediately extracted ($n = 3$/group). Homogenates of the ipsilateral hemisphere were serially processed for Western blotting, as described previously (Jung et al., 2004; Lee et al., 2006). We used anti-eNOS (1:200; BD Biosciences PharMingen, San Diego, CA), anti-COX2 (1:200; BD Biosciences PharMingen), anti-PPARγ (1:1000; Santa Cruz Biotechnology, Inc., Santa Cruz, CA), and anti-β-actin antibody (Santa Cruz Biotechnology, Inc.). Relative optical densities were obtained via comparison of the measured values, with the mean value of the ICH-only group. For PPARγ, cytosolic and nuclear extracts were obtained. Tissues were homogenized with 300 μl of buffer (10 mM *N*-2-hydroxyethylpiperazine-*N'*-2-ethanesulfonic acid, pH 7.9, 1 mM EDTA, 1 mM EGTA, 10 mM KCl, 1 mM dithiothreitol, 0.5 mM phenylmethylsulfonyl fluoride, 0.1 μg/ml aprotinin, 1 μg/ml leupeptin, 1 μg/ml *N*α-*p*-tosyl-L-lysine-chloromethyl ketone, 5 mM NaF, 1 mM NaVO$_4$, 0.5 M sucrose, and 10 mM Na$_2$MoO$_4$). After 15 min, Nonidet P-40 (Roche, Indianapolis, IN) was added to reach a 0.5% concentration. The tubes were gently vortexed for 15 s, and nuclei were collected by centrifugation at 8000*g* for 5 min. Supernatants were taken as a cytosolic fraction. The pellets were resuspended in 100 μl of buffer supplemented with 20% glycerol and 0.4 M KCl, and then they were gently shaken for 30 min at 4°C. Nuclear protein extracts were obtained by centrifugation at 13,000*g* for 5

min, and aliquots of the supernatant were stored at −80°C. All steps of the fractionation were carried out at 4°C.

Reverse Transcription-Polymerase Chain Reaction. We also conducted RT-PCR for Fas, FasL, TNF-α, and the AT1/AT2 receptors (n = 3/group). The following primer sets were used (25 cycles of 95, 58, and 72°C for 40 s each): Fas, 5′-CAA GGG ACT GAT AGC ATC TTT GAG G-3′ (sense) and 5′-TCC AGA TTC AGG GTC ACA GGT TG-3′ (antisense); FasL, 5′-CAG CCC CTG AAT TAC CCA TGT C-3′ (sense) and 5′-CAC TCC AGA GAT CAA AGC AGT TC-3′ (antisense); TNF-α, 5′-TAC TGA ACT TCG GGG TGA TTG GTC C-3′ (sense) and 5′-CAG CCT TGT CCC TTG AAG AGA ACC-3′ (antisense); AT1, 5′-AGA GCC GCA ACA TGA ACT CT-3′ (sense) and 5′-CTG CAT AAG GCG GTT GGT AT-3′ (antisense); and AT2, 5′-AAT CTG GCT GTG GCT GAC TT-3′ (sense) and 5′-AAG GAA GTG CCA GGT CAA TG-3′ (antisense). The mRNA expression levels were normalized to glyceraldehyde-3-phosphate dehydrogenase, and relative optical densities were determined via comparison of the measured values with the mean value of the ICH-only group.

Measurement of Caspase Activities. Caspase activities were characterized with enzyme-linked immunosorbent assay kits (caspase-3; Promega, Madison, WI; caspase-8; BD Biosciences, San Jose, CA; and caspase-9, Chemicon International; n = 3/group) at 24 h after the induction of ICH, as was described previously in other reports (Lee and Lo, 2003). Fluorescent intensity was measured in an FL600 plate reader (excitation wavelength, 380 nm; emission wavelength, 460 nm; Bio-Tek, Instruments, Winooski, VT).

Evaluation of Oxidative Stress. One day after reperfusion, the rat brains were processed for the analysis of oxidative stress (n = 6/group). The oxidative fluorescent dye dihydroethidium (DHE; Sigma-Aldrich) was used to evaluate in situ production of superoxide (Jung et al., 2006). Frozen, enzymatically intact brains were cut into 30-μm-thick sections, and the sections were placed on a glass slide. The sections were simultaneously incubated with 10 μM DHE in PBS for 30 min at 37°C in a humidified chamber that was shielded from light. Coronal sections cut through the striatum (three sections per brain; 1 mm in width) were imaged in parallel. Superoxide-positive cells were manually counted in the eight regions around the striatum under 100× magnification using a laser scanning confocal microscopy with a Bio-Rad MRC 1024 (argon and krypton; Bio-Rad, Hercules, CA). Malondialdehyde (MDA) was estimated as an indicator of lipid peroxidation (n = 3/group). The brain tissues were homogenized with sodium phosphate buffer, pH 7.4. The reagents (1.5 ml of acetic acid, 1.5 ml of thiobarbituric acid, and 0.2 ml of sodium dodecyl sulfate) were added to 0.1 ml of processed tissue sample. The mixture was then heated at 100°C for 60 min. The mixture was cooled with tap water, and 5 ml of n-butanol/pyridine (15:1) and 1 ml of distilled water were added. After centrifugation at 4000 rpm for 10 min, the organic layer was withdrawn, and absorbance was measured at 532 nm using a spectrophotometer.

Statistical Analysis. All data in this study are presented as means ± S.D. Data were analyzed by one-way analysis of variance (ANOVA) followed by Tukey's test (when appropriate) or Student's t test if the data were normally distributed (Kolmogorov-Smirov test; p > 0.05). For the blood pressure and behavioral data, values of different time points were compared by two-way repeated measures ANOVA. Without normal distribution, we used the Mann-Whitney U test.

Results

Telmisartan Prompted a Functional Recovery. There were no significant differences in rectal temperature, arterial blood gases, and pH values among the experimental groups measured before and after ICH induction, and 6 and 24 h after telmisartan (or PBS) administration. Post-ICH mean arterial pressure (89.4 ± 5.8 mm Hg) did not significantly differ (p = 0.302) from baseline pressure (87.5 ± 3.0 mm Hg).

Mean arterial blood pressure at 6 h after drug treatment was slightly lower than that after PBS administration, but this did not reach statistical significance (p = 0.218; two-way repeated measures ANOVA). Data are available in Supplemental Table 1. The ICH-TMS group exhibited less profound deficits than did the ICH-only group at 1 day after the induction of ICH, and then it continued to recover, with the difference between the two groups statistically significant until at least 4 weeks after the induction of ICH (p < 0.05; t test). At week 4, the ICH-TMS group scored less than 2 points on the MLPT (Fig. 1a).

Telmisartan Reduced Hemorrhage Volume and Brain Water Content. Telmisartan treatment attenuated the hemorrhage volume by 63%, compared with the ICH-only group, 1 day after the induction of ICH, and by 86% at 3 days after ICH. The hemorrhage volumes were as follows: 43.4 ± 4.5 μl (day 1) and 22.5 ± 4.5 μl (day 3) in the ICH-only group; and 16.2 ± 2.5 μl (day 1) and 3.1 ± 0.7 μl (day 3) in the ICH-TMS group (p < 0.01, t test; Fig. 1b). Brain water content in the lesioned (left) hemisphere was 81.81 ± 0.59% in the ICH-only group and 79.96 ± 0.41% in the ICH-TMS group, with a significant difference (p < 0.01, t test; Fig. 1c). Brain water content in the nonlesioned (right) hemisphere was 79.51 ± 0.56% in the ICH-only group and 79.47 ± 0.25% in the ICH-TMS group (p = 0.88, t test). We also investigated the effect of telmisartan on brain water content in the autologous blood-injected ICH model, in which similar patterns of brain water content decrement were observed. In this model, the brain water contents of the hemorrhagic hemispheres were 80.8 ± 0.84% in the ICH-only group and 79.42 ± 0.86% in ICH-TMS (p < 0.01, t test; Fig. 1d).

Telmisartan Reduced Inflammatory Cell Infiltration and Apoptotic Cells. TUNEL staining revealed a high density of positively stained cells within the hemorrhage lesions themselves as well as in the periphery of the lesions (Fig. 2a). Quantitative analysis revealed differences between the groups with regard to the number of TUNEL$^+$ cells. The ICH-TMS group exhibited a significantly lower number of TUNEL$^+$ cells (29.28 ± 5.98 cells/mm^2) than did the ICH-only group (336.48 ± 26.27 cells/mm^2; p < 0.01, t test; Fig. 2b). The ICH-TMS group was determined to possess significantly lower numbers of OX42$^+$ microglial cells (ICH-TMS, 24.19 ± 6.10 cells/mm^2; ICH-only, 90.28 ± 10.71 cells/mm^2; p < 0.01, t test) and MPO$^+$ neutrophils (ICH-TMS, 71.57 ± 20.87 cells/mm^2; ICH-only, 195.84 ± 15.29 cells/mm^2; p < 0.01, t test) than were observed in the ICH-only group at 3 days after ICH (Fig. 2b).

Telmisartan Down-Regulated the Inflammatory and Apoptotic Molecules, Combined with the Up-Regulation of eNOS Expression and PPARγ. Western blotting revealed the up-regulation of PPARγ and eNOS expression and the down-regulation of COX2 induced by telmisartan treatment (Fig. 3a). Analysis of the 52-kDa band corresponding to PPARγ demonstrated a 1.6 ± 0.1-fold increase in nuclear extracts of hemorrhagic brain tissue at 24 h after the onset of ICH, while it showed no differences in cytosolic extracts (Fig. 3, b and c). The relative optical density of eNOS expression in the ICH-TMS group was 16.5 ± 1.2 times as high as in the ICH-only group (p < 0.01, Mann-Whitney U test; Fig. 3d). Meanwhile, COX2 expression was significantly attenuated in the ICH-TMS group (35% decrease versus ICH-only group; p < 0.01, Mann-Whitney U test; Fig. 3e).
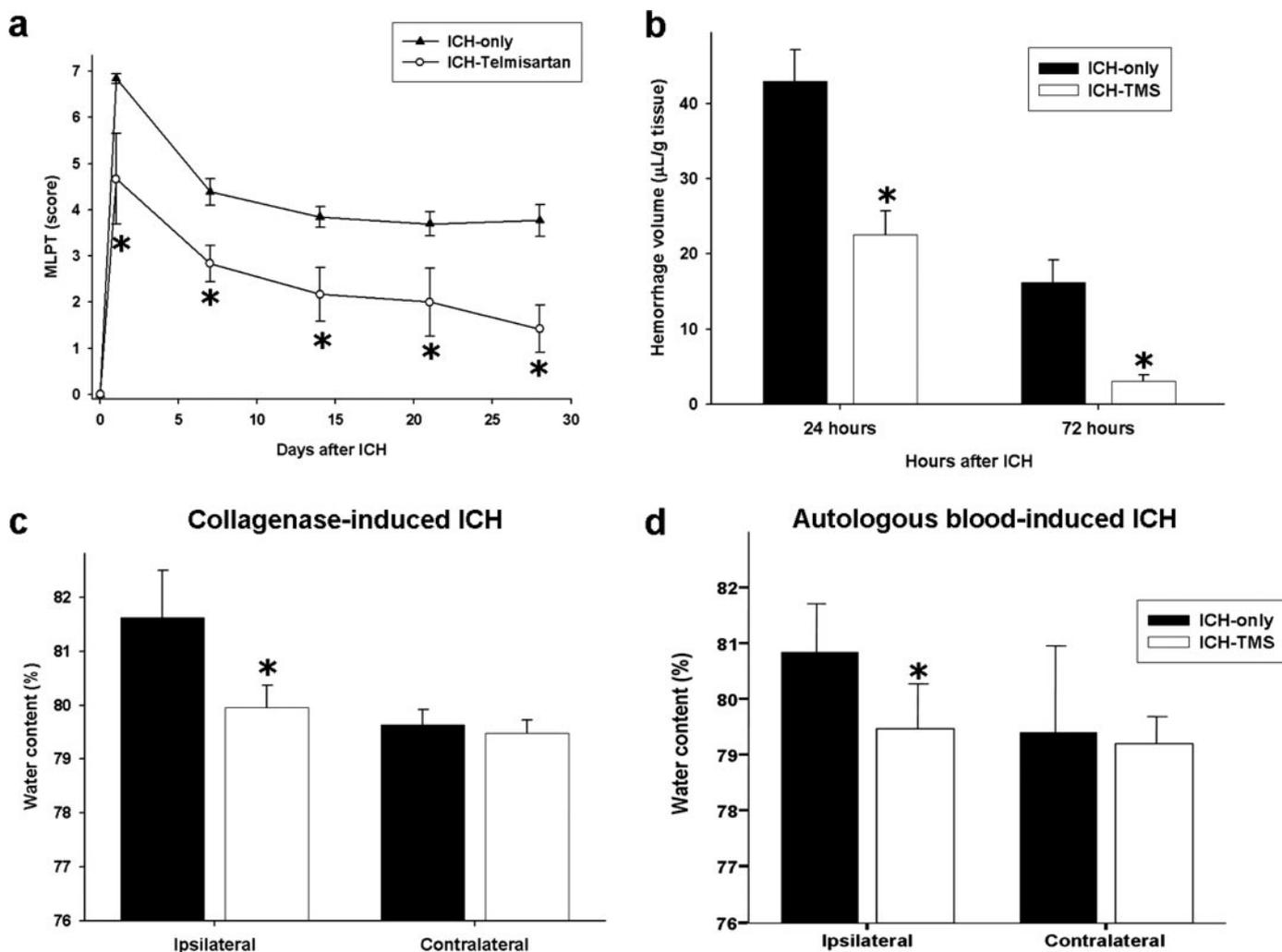
Fig. 1. Behavioral test, hemorrhage volume, and brain water content. a, in the MLPT, the ICH-TMS group exhibited less pronounced initial deficits, and it recovered better than did the ICH-only group. b, telmisartan reduced the hemorrhage volume by 55% at 24 h and by 83% at 72 h compared with the ICH-only group. Telmisartan significantly reduced brain water contents on the ipsilateral side following collagenase-induced ICH (c) and autologous blood-induced ICH (d), compared with what was observed in the ICH-only group at 72 h (c). *, $p < 0.05$ versus ICH-only ($n = 6$; t test).
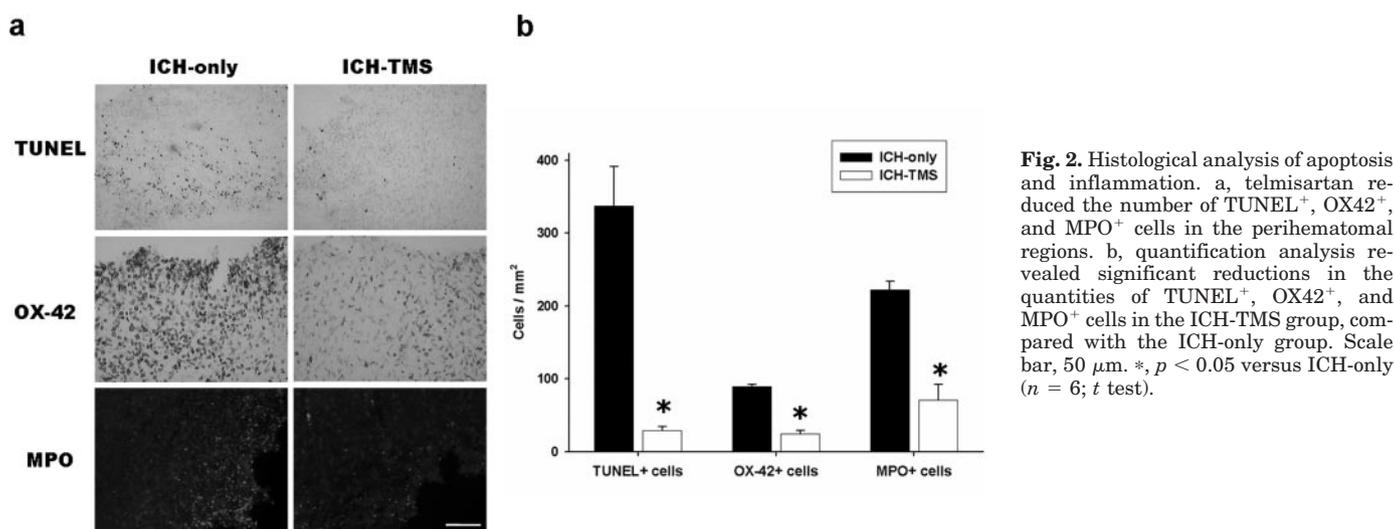
Fig. 2. Histological analysis of apoptosis and inflammation. a, telmisartan reduced the number of TUNEL[+], OX42^{+}, and MPO^{+} cells in the perihematomal regions. b, quantification analysis revealed significant reductions in the quantities of TUNEL[+], OX-42^{+}, and MPO^{+} cells in the ICH-TMS group, compared with the ICH-only group. Scale bar, 50 μm. *, $p < 0.05$ versus ICH-only ($n = 6$; t test).

Caspase activities were significantly reduced in the ICH-TMS group. Twenty-four hours after the induction of ICH, caspase-3 activity in the ICH-TMS group was determined to be significantly lower than that of the ICH-only group (62%

decrease; $p < 0.01$, Mann-Whitney U test; Fig. 3f). Caspase-8 and -9 activities were also shown to have been significantly reduced in the ICH-TMS group (31% decrease in caspase-8; 20% decrease in caspase-9; $p < 0.01$, t test; Fig. 3f). In the
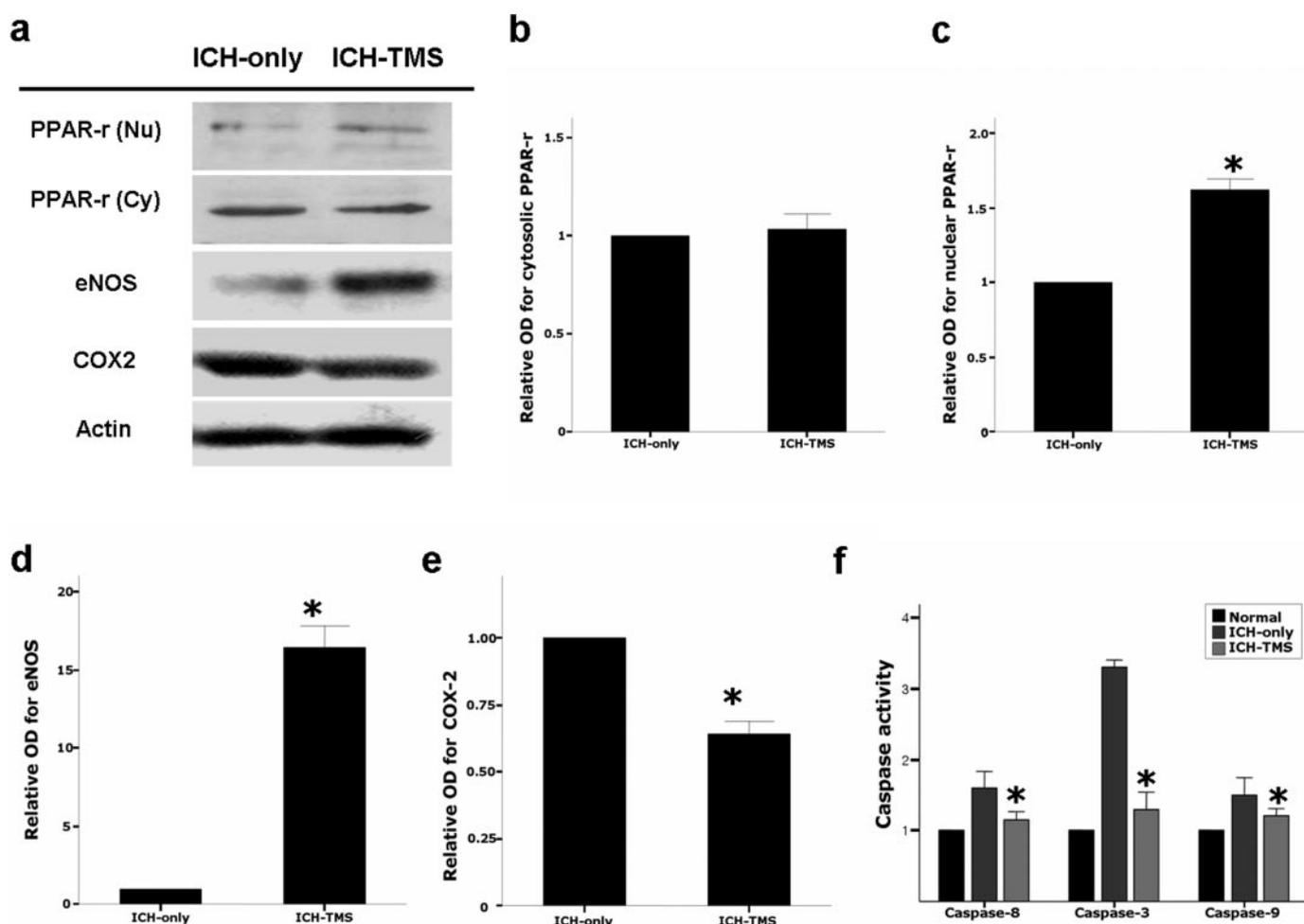
Fig. 3. Western blotting and caspase activity assay. Western blotting (a) revealed the nuclear and cytosolic fractions of PPARγ, eNOS, and COX2 expression. Densitometric analysis of the band (b–e) indicated an increase in the nuclear fraction of PPARγ and eNOS expression and a decrease in the COX2 expression in the ICH-TMS group. Telmisartan significantly reduced the activity of all of the tested caspases, caspase-8, caspase-9, and caspase-3 (f). The densitometric data are representative of three experiments. ∗, $p < 0.0$ versus ICH-only ($n = 3$; Mann-Whitney U test).

analysis for the angiotensin II receptors AT1 and AT2, both of the ICH groups manifested marked increases in the expression of AT1 receptor mRNA after injury (3.5-fold increase, ICH-only; 3.1-fold increase, ICH-TMS), but they exhibited no changes in the expression of the AT2 receptor (Fig. 4, a and b). We measured the mRNA expression of cytokine-related genes, including TNF-α, Fas, and FasL. The hemorrhagic brain samples expressed abundant amounts of mRNA of these molecules, whereas the normal brains expressed them only at very low levels. Relative optical density analysis revealed the ICH-TMS group to have undergone a 94% decrease in the levels of TNF-α, a 56% decrease in Fas, and a 79% reduction in FasL mRNA levels, compared with the ICH-only group ($p < 0.01$, Mann-Whitney U test; Fig. 4c).

Telmisartan Reduced Oxidative Stress in the Hemorrhagic Brain. In the normal rats, limited evidence of DHE-induced ethidium bromide fluorescence was observed in the cortex and striatum. Superoxide-generating cells were increased in the hemorrhagic hemisphere, whereas only a few labeled cells were detected in the nonhemorrhagic hemisphere (Fig. 5, a–c). Data from image analysis indicated that DHE-induced ethidium bromide fluorescence was 74% less pronounced in the ICH-TMS group than in the ICH-only group ($p < 0.05$, t test; Fig. 5d). These histological results

were further supported by biochemical assay for MDA, a lipid peroxidation product. Telmisartan significantly decreased the levels of MDA (0.16 ± 0.04 μg/mg protein) compared with the ICH-only group (0.31 ± 0.05 μg/mg protein) and normal group (0.07 ± 0.03 μg/mg protein) ($p < 0.05$, Mann-Whitney U test; Fig. 5e).

Discussion

In this study, telmisartan was shown to attenuate hemorrhage expansion and perihematomal edema formation, to induce neuroprotection, and to enhance functional recovery. These effects of telmisartan were associated with the inhibition or amelioration of apoptosis, oxidative stress, and neuroinflammation, rather than blood pressure reduction.

The dose (30 mg/kg p.o.) used in this study was selected on the basis of pharmacokinetic study in the brain (Gohkle et al., 2001). Telmisartan concentrations measured in the cerebrospinal fluid after 8 days of consecutive daily oral treatment (1–30 mg/kg) ranged from 0.87 ± 0.27 ng/ml (1 mg/kg/dose) to 46.5 ± 11.6 ng/ml (30 mg/kg/dose). Following peripheral administration, telmisartan can penetrate the BBB in a dose- and time-dependent manner to inhibit centrally mediated effects of angiotensin II. Compared with lo-
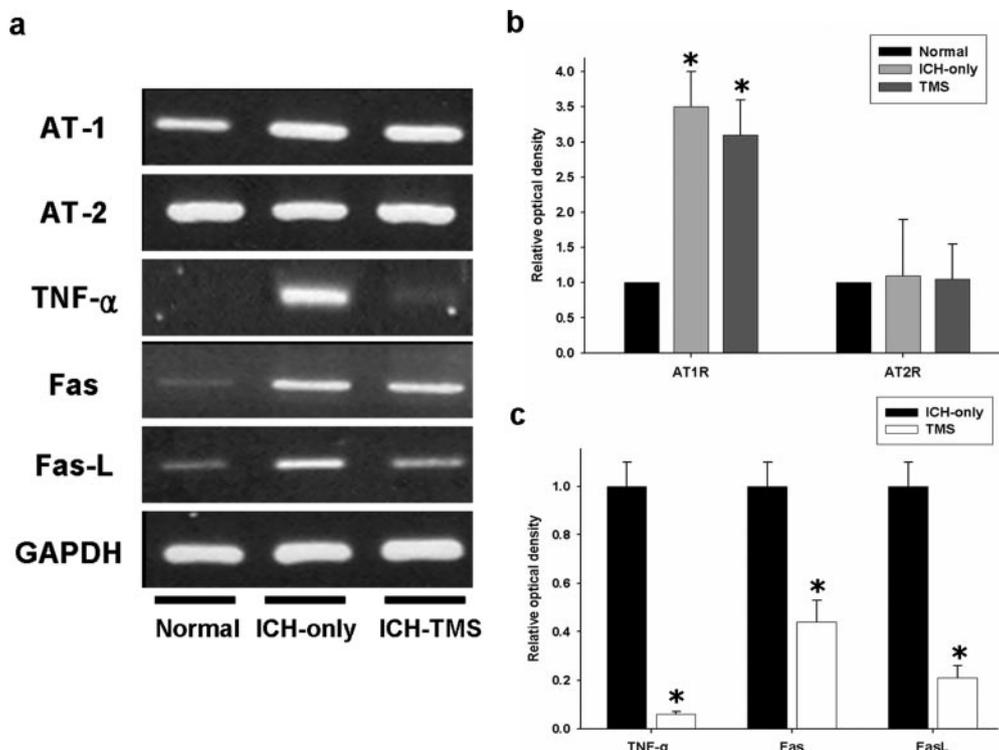
Fig. 4. RT-PCR for AT1, AT2, TNF-α, Fas, and FasL expression. a, RT-PCR results were analyzed in terms of the optical density ratio to the glyceraldehyde-3-phosphate dehydrogenase. b, AT1 was up-regulated in the hemorrhagic compared with the normal samples, and this was also apparent in the ICH-TMS group. However, AT2 exhibited no changes. c, whereas the ICH-only group exhibited up-regulations in TNF-α, Fas, and FasL, the ICH-TMS rats exhibited reduced expressions of all of these molecules. ∗, $p < 0.05$ versus normal in b and versus ICH-only in c ($n = 3$; Mann-Whitney U test).
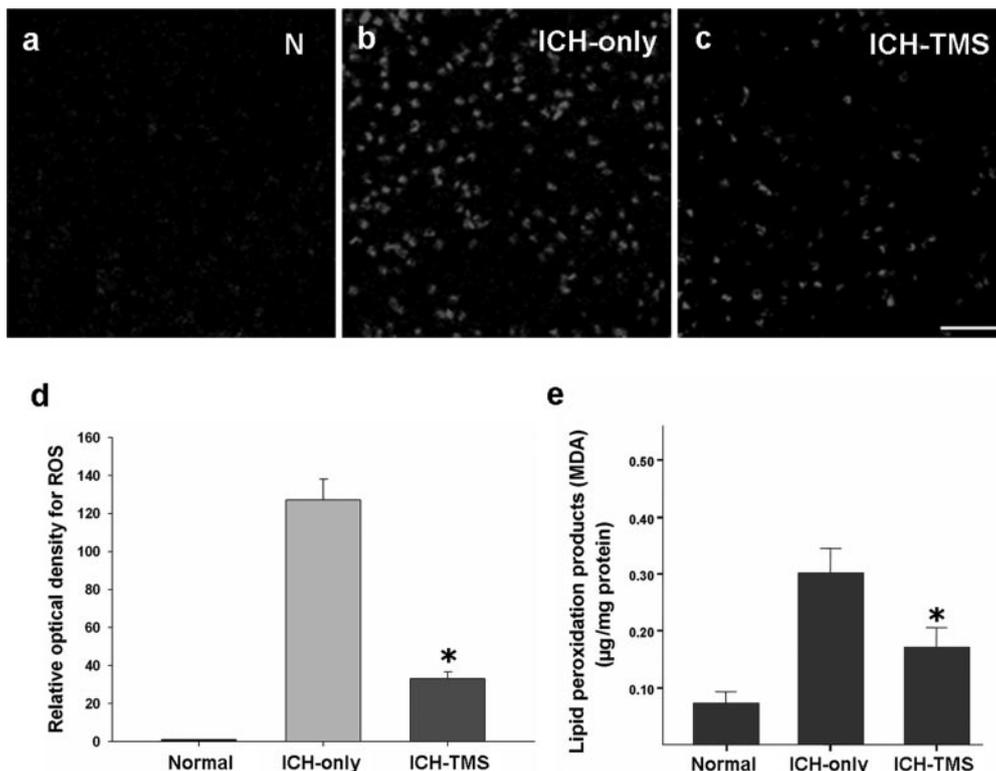
Fig. 5. Antioxidant effects of telmisartan. Fluorescent images after incubation with DHE demonstrated that basal superoxide levels were increased in the hemorrhagic brains and that telmisartan treatment effected a reduction in the DHE fluorescence, which indicated reduced superoxide generation (a–c). Quantitative measurements of DHE fluorescence (d) indicated a 74% decrease in the ICH-TMS group, compared with the ICH-only group. Scale bar, 50 μm. ∗, $p < 0.01$ versus ICH-only ($n = 6$; ANOVA and Tukey's test). Telmisartan significantly decreased the elevated MDA content in rat brain after ICH (e). ∗, $p < 0.05$ versus ICH-only ($n = 3$; Mann-Whitney U test).

sartan and irbesartan, the apparent higher capability of telmisartan to penetrate into the brain tissue might be explained by the hydrophobic/hydrophilic properties of the drugs. Thus, we selected telmisartan (30 mg/kg/dose) as a potential drug against experimental ICH.

The AT1R mRNA level was shown to be increased in the hemorrhagic brain 24 h after ICH induction, whereas mRNA level of the AT2R was not affected. Therefore, it is conceivable to assume that the inhibition of central AT1R can considerably contribute to the observed beneficial effects of the telmisartan on neurological outcome of ICH. In a study involving heart transplantation donors, the systemic up-regulation of AT1R was documented with the subsequent development of transplant vasculopathy and ICH (Yamani et al., 2004). The increased AT1R expression in the hemorrhagic brain, as was documented in our study, suggests its patho-

genetic implication in ICH, and it provides the feasibility of the AT1R blockers. Alternatively, when AT1 receptors are inhibited, angiotensin II can increasingly interact with AT2 receptors, because telmisartan selectively blocks the AT1 receptors and it allows the angiotensin II to stimulate the unoccupied AT2 receptors (Iwai et al., 2004). This dual effect of telmisartan may be the cause of their superiority over the angiotensin-converting enzyme inhibitors in ICH treatment. Evidence has been more recently gathered, suggesting that the stimulation of AT2R can offset or oppose, by cross-talk mechanisms, the AT1-mediated actions of angiotensin II on blood pressure regulation, vascular reactivity, cell growth, and apoptosis (Wright et al., 2002; Wu et al., 2002). The relative stimulation of the AT2R, as an indirect result of AT1R antagonism, may contribute to the overall effects of the AT1R antagonists during pathophysiological process of ICH. However, the relationship between telmisartan and AT receptor subtype is not necessarily straightforward, and it warrants further study.

The inhibition of AT1R induces eNOS expression in injured tissue via the activation of AT2R (Thai et al., 2003). The telmisartan-induced activation of eNOS may perform a function relevant to the preservation of cerebral blood flow and the attenuation of neurological loss in the perihematomal regions (Endres et al., 2004; Jung et al., 2004). In addition, nitric oxide from eNOS can be protective against oxidative stress and excitotoxic damage (Iadecola, 1997; Agnoletti et al., 1999), and it can reduce brain edema (Lee et al., 2006). However, nitric oxide might aggravate the ICH conditions via inhibiting platelet activation and preventing thrombosis (Stagliano et al., 1997). Additional genetic controls, including pharmacologic blocking, or genetic knockdown of eNOS, would be helpful to verify a role of telmisartan-induced eNOS.

Apoptosis represents a prominent feature of ICH-associated cell death in the perihematomal region (Qureshi et al., 2003). In cells responsive to apoptotic stimuli, two major apoptosis pathways have been identified: the intrinsic apoptotic pathway, which includes mitochondria-involved signaling and caspase-9; and the extrinsic apoptotic pathway, which is mediated principally by death receptors and caspase-8 (Qureshi et al., 2003; Huang et al., 2004). Since telmisartan attenuated the activities of caspase-9, caspase-3, and caspase-8, and the mRNA levels of FasL and TNF-α, we speculate that telmisartan can alleviate both the intrinsic and extrinsic apoptotic pathway activation associated with ICH. Conversely, a variety of experimental and human studies regarding ICH has revealed that inflammation can be a major target of novel therapies for ICH (Chu et al., 2004; Jung et al., 2004; Lee et al., 2006). In line with reports that some ARBs exerted anti-inflammatory effects (Krämer et al., 2002; Nagai et al., 2006), telmisartan in our study could inhibit the number of infiltrating leukocytes and activated microglia, and the expression of COX2 in the hemorrhagic brain. Oxidative stress during ICH is another critical event, which leads to the disruption of the BBB, combined with hematoma expansion and secondary vasogenic edema (Tang et al., 2005). Angiotensin II is one of the most important known oxidative stress inducers, and produce reactive oxygen species by the enzyme NADPH oxidase (Cai et al., 2003). The reduced levels of the superoxide and lipid peroxidation

product by telmisartan might contribute to a remarkable reduction in the hematoma growth and edema.

Recent evidence suggests that PPARγ activation represents a novel mechanism for the beneficial effects of ARBs (Benson et al., 2004; Schupp et al., 2004). Telmisartan can function as a partial agonist of PPARγ (Benson et al., 2004). The ability of telmisartan to activate PPARγ seems to be independent of AT1R blockade, because it can activate PPARγ in cells that lack AT1R (Schupp et al., 2004). PPARγ activators can ameliorate multiple pathogenetic determinants of atherosclerosis, ischemia, or inflammation (Schiffrin et al., 2003). Thus, some interest exists in the potential use of PPARγ activators for treatment of ICH. In our study, the administration of telmisartan at the onset of ICH coincided with the activation of PPARγ and suppression of inflammation and oxidative stress. The PPARγ activation induces catalase gene expression and protein. The inducibility of the catalase gene could play an important role in combating the oxidative stress induced by ICH (Nakamura et al., 2005). It has also been postulated that the beneficial effect of PPARγ agonists in stroke is because of their anti-inflammatory effect. Most of the proinflammatory responses are amplified and regulated by the transcription factor NF-κB. PPARγ agonists have been shown to inhibit NF-κB, either directly by interacting with its subunits, by competing for common transcription coactivators, or through up-regulation of its inhibitory protein, inhibitor κBa (Delerive et al., 2000). In a recent study, 15-deoxy-^{12,14}Á-prostaglandin-J2, a PPARγ agonist, could elevate the catalase expression and suppress the NF-κB activity, and it could restrict neutrophil infiltration (Zhao et al., 2006). Therefore, it is likely that the up-regulation of PPARγ by telmisartan, as shown in the present study, may provide an explanation for the antioxidative and anti-inflammatory effects of telmisartan. By virtue of its unique ability to activate PPARγ at reasonable concentrations, telmisartan may have a greater potential than other ARBs to improve the hostile environments of the hemorrhagic brain.

In conclusion, we provide convincing evidence to suggest that telmisartan does indeed exert therapeutic effects in experimental ICH. Telmisartan is widely used in the current clinical field, as an antihypertensive agent. Considering that the use of antihypertensive agents in ICH patients is seldom contraindicated, the clinical use of telmisartan in cases of ICH may be an option with a fair degree of feasibility.

References

Ando H, Zhou J, Macova M, Imboden H, and Saavedra JM (2004) Angiotensin II AT1 receptor blockade reverses pathological hypertrophy and inflammation in brain microvessels of spontaneously hypertensive rats. *Stroke* **35:**1726–1731.

Agnoletti L, Curello S, Bachetti T, Malacarne F, Gaia G, Comini L, Volterrani M, Bonetti P, Parrinello G, Cadei M, et al. (1999) Serum from patients with severe heart failure downregulates eNOS and is proapoptotic: role of tumor necrosis factor-alpha. *Circulation* **100:**1983–1991.

Benson SC, Pershadsingh HA, Ho CI, Chittiboyina A, Desai P, Pravenec M, Qi N, Wang J, Avery MA, and Kurtz TW (2004) Identification of telmisartan as a unique angiotensin II receptor antagonist with selective PPARγ-modulating activity. *Hypertension* **43:**993–1002.

Cai H, Griendling KK, and Harrison DG (2003) The vascular NAD(P)H oxidases as therapeutic targets in cardiovascular diseases. *Trends Pharmacol Sci* **24:**471–478.

Chalupsky K and Cai H (2005) Endothelial dihydrofolate reductase: critical for nitric oxide bioavailability and role in angiotensin II uncoupling of endothelial nitric oxide synthase. *Proc Natl Acad Sci U S A* **102:**9056–9061.

Chu K, Jeong SW, Jung KH, Han SY, Lee ST, Kim M, and Roh JK (2004) Celecoxib induces functional recovery after intracerebral hemorrhage with reduction of brain edema and perihematomal cell death. *J Cereb Blood Flow Metab* **24:**926–933.

Dai WJ, Funk A, Herdegen T, Unger T, and Culman J (1999) Blockade of central angiotensin AT(1) receptors improves neurological outcome and reduces expression of AP-1 transcription factors after focal brain ischemia in rats. *Stroke* **30:**2391–2398.

Delerive P, Gervois P, Fruchart JC, and Staels B (2000) Induction of IκBα expression as a mechanism contributing to the anti-inflammatory activities of peroxisome proliferator-activated receptor-α activators. *J Biol Chem* **275:**36703–36707.

Endres M, Laufs U, Liao JK, and MoskowitZ MA (2004) Targeting eNOS for stroke protection. *Trends Neurosci* **27:**283–289.

Gohlke P, Weiss S, Jansen A, Wienen W, Stangier J, Rascher W, Culman J, and Unger T (2001) AT1 receptor antagonist telmisartan administered peripherally inhibits central responses to angiotensin II in conscious rats. *J Pharmacol Exp Ther* **298:**62–70.

Huang DM, Shen YC, Wu C, Huang YT, Kung FL, Teng CM, and Guh JH (2004) Investigation of extrinsic and intrinsic apoptosis pathways of new clerodane diterpenoids in human prostate cancer PC-3 cells. *Eur J Pharmacol* **503:**17–24.

Iadecola C (1997) Bright and dark sides of nitric oxide in ischemic brain injury. *Trends Neurosci* **20:**132–139.

Iadecola C and Gorelick PB (2004) Hypertension, angiotensin, and stroke: beyond blood pressure. *Stroke* **35:**348–350.

Institute of Laboratory Animal Resources (1996) *Guide for the Care and Use of Laboratory Animals* 7th ed. Institute of Laboratory Animal Resources, Commission on Life Sciences, National Research Council, Washington DC.

Ito T, Yamakawa H, Bregonzio C, Terron JA, Falcon-Neri A, and Saavedra JM (2002) Protection against ischemia and improvement of cerebral blood flow in genetically hypertensive rats by chronic pretreatment with an angiotensin II AT1 antagonist. *Stroke* **33:**2297–2303.

Iwai M, Liu HW, Chen R, Ide A, Okamoto S, Hata R, Sakanaka M, Shiuchi T, and Horiuchi M (2004) Possible inhibition of focal cerebral ischemia by angiotensin II type 2 receptor stimulation. *Circulation* **110:**843–848.

Jung KH, Chu K, Jeong SW, Han SY, Lee ST, Kim JY, Kim M, and Roh JK (2004) HMG-CoA reductase inhibitor, atorvastatin, promotes sensorimotor recovery, suppressing acute inflammatory reaction after experimental intracerebral hemorrhage. *Stroke* **35:**1744–1749.

Jung KH, Chu K, Ko SY, Lee ST, Sinn DI, Park DK, Kim JM, Song EC, Kim M, and Roh JK (2006) Early intravenous infusion of sodium nitrite protects brain against in vivo ischemia-reperfusion injury. *Stroke* **37:**2744–2750.

Krämer C, Sunkomat J, Witte J, Luchtefeld M, Walden M, Schmidt B, Boger RH, Forssmann WG, Drexler H, and Schieffer B (2002) Angiotensin II receptor independent antiinflammatory and antiaggregatory properties of losartan: role of the active metabolite EXP3179. *Circ Res* **90:**770–776.

Lee SR and Lo EH (2003) Interactions between p38 mitogen-activated protein kinase and caspase-3 in cerebral endothelial cell death after hypoxia-reoxygenation. *Stroke* **34:**2704–2709.

Lee ST, Chu K, Sinn DI, Jung KH, Kim EH, Kim SJ, Kim JM, Ko SY, Kim M, and Roh JK (2006) Erythropoietin reduces perihematomal inflammation and cell death with eNOS and STAT3 activations in experimental intracerebral hemorrhage. *J Neurochem* **96:**1728–1739.

Mayne M, Ni W, Yan HJ, Xue M, Johnston JB, Del Bigio MR, Peeling J, and Power C (2001) Antisense oligodeoxynucleotides inhibition of tumor necrosis factor-alpha expression is neuroprotective after intracerebral hemorrhage. *Stroke* **32:**240–248.

Nagai N, Oike Y, Izumi-Nagai K, Urano T, Kubota Y, Noda K, Ozawa Y, Inoue M, Tsubota K, Suda T, et al. (2006) Angiotensin II type 1 receptor-mediated inflammation is required for choroidal neovascularization. *Arterioscler Thromb Vasc Biol* **26:**2252–2259.

Nakamura T, Keep RF, Hua Y, Hoff JT, and Xi G (2005) Oxidative DNA injury after experimental intracerebral hemorrhage. *Brain Res* **1039:**30–36.

Nishimura Y, Ito T, and Saavedra JM (2000) Angiotensin II AT(1) blockade normalizes cerebrovascular autoregulation and reduces cerebral ischemia in spontaneously hypertensive rats. *Stroke* **31:**2478–2486.

Peeling J, Yan HJ, Corbett D, Xue M, and Del Bigio MR (2001) Effect of FK-506 on inflammation and behavioral outcome following intracerebral hemorrhage in rat. *Exp Neurol* **167:**341–347.

Qureshi AI, Suri MF, Ostrow PT, Kim SH, Ali Z, Shatla AA, Guterman LR, and Hopkins LN (2003) Apoptosis as a form of cell death in intracerebral hemorrhage. *Neurosurgery* **52:**1041–1047.

Rajagopalan S, Kurz S, Munzel T, Tarpey M, Freeman BA, Griendling KK, and Harrison DG (1996) Angiotensin II-mediated hypertension in the rat increases vascular superoxide production via membrane NADH/NADPH oxidase activation. Contribution to alterations of vasomotor tone. *J Clin Invest* **97:**1916–1923.

Schiffrin EL, Amiri F, Benkirane K, Iglarz M, and Diep QN (2003) Peroxisome proliferator-activated receptors: vascular and cardiac effects in hypertension. *Hypertension* **42:**664–668.

Schupp M, Janke J, Clasen R, Unger T, and Kintscher U (2004) Angiotensin type 1 receptor blockers induce peroxisome proliferator-activated receptor-gamma activity. *Circulation* **109:**2054–2057.

Stagliano N, Zhao W, Prado R, Dewanjee M, Ginsberg M, and Dietrich W (1997) The effect of nitric oxide synthase inhibition on acute platelet accumulation and hemodynamic depression in a rat model of thromboembolic stroke. *J Cereb Blood Flow Metab* **17:**1182–1190.

Tang J, Liu J, Zhou C, Ostanin D, Grisham MB, Neil Granger D, and Zhang JH (2005) Role of NADPH oxidase in the brain injury of intracerebral hemorrhage. *J Neurochem* **94:**1342–1350.

Thai H, Wollmuth J, Goldman S, and Gaballa M (2003) Angiotensin subtype 1 receptor blockade improves vasorelaxation in heart failure by up-regulation of endothelial nitric-oxide synthase via activation of the AT2 receptor. *J Pharmacol Exp Ther* **307:**1171–1178.

Walther T, Olah L, Harms C, Maul B, Bader M, Hortnagl H, Schultheiss H, and Mies G (2002) Ischemic injury in experimental stroke depends on angiotensin II. *FASEB J* **16:**169–176.

Wang X, Mori T, Sumii T, and Lo EH (2002) Hemoglobin-induced cytotoxicity in rat cerebral cortical neurons: caspase activation and oxidative stress. *Stroke* **33:**1882–1888.

Wright JW, Reichert JR, Davis CJ, and Harding JW (2002) Neural plasticity and the brain renin-angiotensin system. *Neurosci Biobehav Rev* **26:**529–552.

Wu L, Iwai M, Nakagami H, Chen R, Suzuki J, Akishita M, de Gasparo M, and Horiuchi M (2002) Effect of angiotensin II type 1 receptor blockade on cardiac remodeling in angiotensin II type 2 receptor null mice. *Arterioscler Thromb Vasc Biol* **22:**49–54.

Yamakawa H, Jezova M, Ando H, and Saavedra JM (2003) Normalization of endothelial and inducible nitric oxide synthase expression in brain microvessels of spontaneously hypertensive rats by angiotensin II AT1 receptor inhibition. *J Cereb Blood Flow Metab* **23:**371–380.

Yamani MH, Cook DJ, Tuzcu EM, Abdo A, Paul P, Ratliff NB, Yu Y, Yousufuddin M, Feng J, Hobbs R, et al. (2004) Systemic up-regulation of angiotensin II type 1 receptor in cardiac donors with spontaneous intracerebral hemorrhage. *Am J Transplant* **4:**1097–1102.

Zhao X, Zhang Y, Strong R, Grotta JC, and Aronowski J (2006) 15d-Prostaglandin J2 activates peroxisome proliferator-activated receptor-gamma, promotes expression of catalase, and reduces inflammation, behavioral dysfunction, and neuronal loss after intracerebral hemorrhage in rats. *J Cereb Blood Flow Metab* **26:**811–820.

Zhou J, Ando H, Macova M, Dou J, and Saavedra JM (2005) Angiotensin II AT1 receptor blockade abolishes brain microvascular inflammation and heat shock protein responses in hypertensive rats. *J Cereb Blood Flow Metab* **25:**878–886.

Address correspondence to: Dr. Jae-Kyu Roh, Department of Neurology, Seoul National University Hospital, 28, Yongon-Dong, Chongro-Gu, Seoul, 110-744, Republic of Korea. E-mail: rohjk@snu.ac.kr